Jordan Journal of Civil Engineering, Volume **17**, No. **4**, **2023**
DOI: https://doi.org/10.14525/JJCE.v17i4.01

Mechanical Properties of Slab Ballastless Track Subjected to Combined Effects of Loading and Temperature

Guowen Yao [1), 2)], ***Anxiang Song*** [1)*], ***Shiya Li*** [1)], ***Rui Zhou*** [3)], ***Gaofeng Zhang*** [2)], ***Shuhang Wu*** [2)]

[1)] State Key Laboratory of Mountain Bridge and Tunnel Engineering, Chongqing Jiaotong University, Chongqing 400074, China.
[2)] School of Civil Engineering, Chongging Jiaotong University, Chongqing 400074, China.
* Corresponding Author. E-Mail: 1225763598@qq.com
[3)] College of Civil and Transportation Engineering, Shenzhen University, Shenzhen 518060, China

ABSTRACT

Temperature has a significant impact on the structural performance of the China Railway Track System (CRTS) II slab ballastless track-bridge and the structure is susceptible to fatigue damage under long-term loading. Therefore, it is crucial to conduct cyclic-loading test on the track-bridge structure to reveal the evolution of its mechanical properties under coupled temperature-load effect. In this study, a 1:4 scaled-down model of a ballastless track-bridge was produced and placed in a large-size environmental chamber for temperature-load coupled cyclic-loading tests. The results showed that after 1×10^6 cycles of loading, no cracks were observed on the surface of the track structure. The structural workability and load capacity of the track-bridge met the required service standards. During the temperature-load coupling test, the load-displacement curves of the structural system exhibited intervals, with a more significant increase in static-deflection values. The dynamic deflection of the structural system under the coupling action experienced a higher growth rate and more abrupt changes compared to single-load conditions. These observations indicated that the ambient temperature amplified the deflection of the structural system. The strain values in the track structure exhibited significant non-linearity, with temperature amplifying this effect. The dynamic-response test results revealed a negative correlation between the inherent frequency of the track structure and the ambient temperature, further emphasizing the influence of temperature on the stability of the track structure. Consequently, it is essential to enhance the monitoring of track structures in high-temperature climates to ensure their safe operation.

KEYWORDS: CRTS II slab ballastless track, Temperature-load coupling, Mechanical properties, Dynamic response.

INTRODUCTION

The CRTS II ballastless track-bridge has been widely used in China's high-speed railway construction because of its good stability and comfort. For example, Beijing-Shanghai high-speed railway bridge accounted for 80.47% of the line (Liu et al., 2019; Feng et al., 2019; Jiang et al., 2019; Song et al.,2023). The CRTS II ballastless track-bridge is a multi-layer heterogeneous structure which mainly consists of track slab, cement asphalt (CA) mortar layer, concrete base, wide-narrow joints and simply-support bridge, as shown in Fig. 1. China is a vast country with a complex ballastless track service environment and intensive high-speed rail operations. Studies have shown that temperature and dynamic train load had the greatest long-term and most severe external effects on ballastless track while in service (Zhu et al., 2014; Li et al., 2019). The impact of the train load produces an effect similar to slapping at the interlayer seam of the track structure, exacerbating interlayer damage to the track structure and destroying the overall integrity of the track structure. The problem of the ballastless-track instability under the coupled

Received on 16/2/2023.
Accepted for Publication on 10/6/2023.

effects of temperature and train load is becoming increasingly prominent.

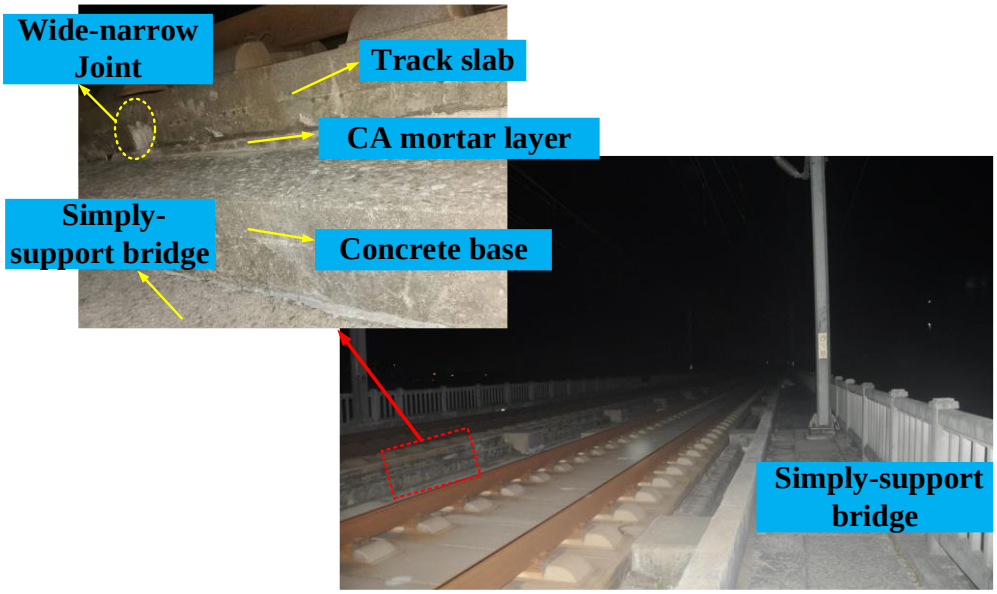

Figure (1): CRTS II ballastless track-bridge utilized in the high-speed railway in China

At present, research on ballastless tracks mainly focuses on the effect of temperature and train loading on the mechanical properties of ballastless tracks. Studies are concentrated on the temperature field and its effect. For example, Ou et al. (2014) derived the vertical temperature distribution function of the ballastless track by considering actual observed values of the outer surface of the track slab and their dependence on the initial conditions and calculated the corresponding values of the structural temperature change with time through theoretical analysis. Wang et al. (2019) and Yang et al. (2017) established a three-dimensional computational model of track temperature field considering track structure direction and geographical location to analyze the temperature characteristics of ballastless tracks under continuous high-temperature weather. Lou et al. (2018) modeled the temperature action of ballastless tracks on bridges and used Fourier series to fit the distribution law of the uniform temperature spectrum to obtain the mapping relationship between the structure and the temperature of the atmosphere. Chen et al. (2019) derived the analytical expression of track slab warpage based on the equilibrium differential equation to obtain the displacement field distribution during the deformation of the track structure. In addition, related scholars carried out indoor temperature load tests on the track structure and conducted an in-depth investigation of the change law of the mechanical properties of the track structure (Zhou et al., 2022; Song et al., 2022; Zhao et al., 2021; Zhou et al., 2020).

On the other hand, a series of studies have been carried out on the mechanical properties of ballastless tracks under train load. To investigate the interfacial bond slip ability and shear resistance of track slab and mortar layer, Dai et al. (2016) conducted field transverse and longitudinal shear load tests on full-size specimens of CRTS II. The tests showed that the bond strength of the interface between track slab and CA mortar layer was much less than that of the interface between CA mortar layer and concrete base and their fracture damage modes were all ductile fracture and put forward the law of interfacial bond slip in this way. Zhang et al. (2021) used a scaled model to carry out static-load tests under the synergistic action of single girders and girder rails to derive the theoretical solutions for deflection and slip of the ballastless track-simply supported girder bridge structural system under vertical static loads in the applicable elastic state. Additionally, Liu et al. (2011) pointed out that the fatigue problem of ballastless tracks is the main field of further exploration. In this regard, Feng et al. (2021) proposed an iterative estimation method for fatigue crack expansion of concrete under long-term dynamic train loading based on the Forman

model and discussed the fatigue crack expansion process and remaining life of the support layer with different initial crack depths. Ren et al. (2019) established a finite-element model based on field tests and theoretical calculations to investigate the effect of passenger and truck operations on the fatigue life of CRTS I track slabs, pointing out that the fatigue life of the track structure is reduced due to the action of trucks. Meanwhile, scholars have proved that the dynamic response of the track has a time effect by using cyclic load and moving train load to load the indoor foot-rule model (Bose et al., 2020; Tarifa et al., 2015). Zeng et al. (2019) used a track-roadbed dynamic loading system and established a foot-rule model to fatigue load the track structure for 30 million cycles, which revealed the evolution of fastener stiffness, vibration isolation layer stiffness and acceleration of the track system. Sheng et al. (2020) conducted fatigue tests for the ballastless track on large-span cable-stayed bridges with foot-rule models, where the results showed that the degradation of ballastless track stiffness under fatigue loading was not significant.

Although the mechanical properties of ballastless tracks under temperature and train loads are investigated, the fatigue properties of track structures underneath the track-bridge structural system need further study. Ballastless tracks in actual service are usually under the combined effect of train load and temperature change and it is difficult to model the actual mechanical response of track structures by considering only the train load. Due to the limitation of the environmental and load coupling loading experimental equipment, there are few experimental studies on coupled temperature and load effects and it is difficult for numerical simulations to truly reflect the long-term mechanical performance of the track structure under the coupled effects. Based on this background, a 1:4 ballastless track-bridge scaled model was produced in the laboratory and a coupled temperature-fatigue load test was performed to study mechanical fatigue during its performance. The research reported in this article reveals the mechanical evolution law of the track structure under coupled temperature-fatigue loading. This can provide some guidance for the maintenance of ballastless track structures and the optimization of track structure design under track-bridge systems.

EXPERIMENTAL PROGRAM

Design and Construction of the Specimen

Considering the boundary conditions and structural continuity, a 32 m prototype structure of CRTS II slab ballastless track-bridge was selected in this paper, which consists of a simple supported girder and CRTS II slab ballastless track. The track structure is composed of track slab, CA mortar layer, concrete base, wide-narrow joint and sliding layer, as shown in Fig. 2. Due to the large size of the prototype structure and the limitation of the testing ground, a similarity ratio of 1:4 was used to scale down the prototype structure and the scale-down parameters are shown in Table 1. The structural materials used in the scaled-down model were kept consistent with those of the prototype structure and the specific material parameters are listed in Table 2. It is worth noting that the adjacent track slabs are connected longitudinally with 20-mm diameter screwed reinforcement to ensure their continuity.

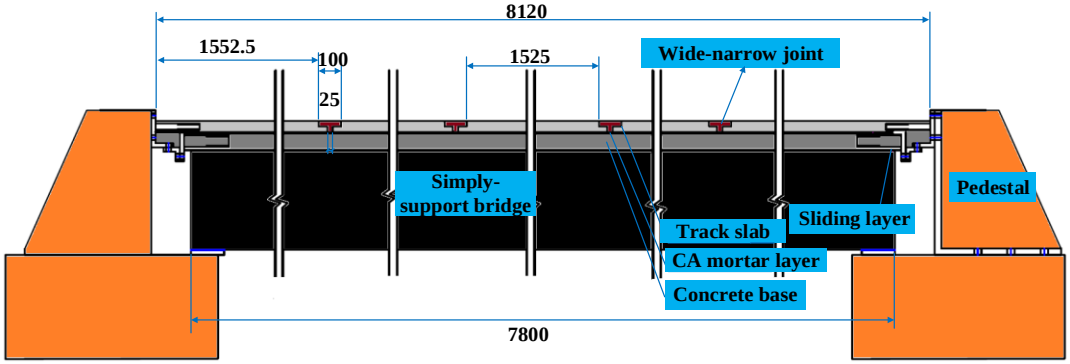

Figure (2): Scaled specimen of CRTS II ballastless track-bridge (uint: mm)

Table 1. The similarity ratio of structural parameters

Main specifications	Scale model	Prototype structure	Prototype structure
Size	L /4	L	L
Density	ρ	ρ	ρ
Elastic modulus	E	E	E
Temperature	T	T	T
Linear expansion coefficient	α	α	α
Vertical bending moment	M/64	M	M
Stress	σ	σ	σ

Table. 2 Material parameters of the specimen

Parts	Material	Poisson's ratio	Elastic modulus（MPa）	Density (kg/m^3)
Track slab/ Wide-narrow joint	C55	0.2	3.55×10^4	2500
Simple box girder	C50	0.2	3.45×10^4	2500
Concrete base	C40	0.2	3.25×10^4	2500
CA mortar layer	Asphalt	0.2	8.0×10^3	2400
Prestressed steel bars	HRB500	0.3	2.1×10^5	7850

Sensors' Layout and Testing Instruments

Strains in both the track slab and concrete base were monitored by FBG (Fiber Bragg Grating) strain sensors and data was collected by a fiber-optic demodulator. The strain sensitivity of the fiber-optic demodulator is 1.6 pm/με, the standard range is ±1500με, the measurement accuracy is taken as less than 0.5% FS and the temperature range of the working environment is -40~120℃. Prior to casting the track slab and the concrete base, the FBG sensor will be bonded to the internal reinforcement surface using super glue and the strain at this point can also be considered as the strain in the concrete. After bonding, a layer of epoxy resin was used on the surface for protection. The detailed location of the light grating sensor is shown in Fig. 3(a).

The vertical relative displacement of the track structure is measured using Linear Variable Displacement Transducer (LVDT). The vertical relative displacement of the track structure was measured by a displacement sensor with a range of 50 mm and an accuracy of 0.5% FS. The static acquisition system was used for acquisition and saved on the computer. The position of the displacement sensor is shown in Fig. 3(b).

Experimental Apparatus

In this paper, the temperature-fatigue load coupling loading test was carried out in the environment/load coupling test system of the State Key Laboratory of Mountain Bridges and Tunnel Engineering from Chongqing Jiaotong University, China. The system consists of a large-scale variable space environment simulation system and a multi-functional servo-dynamic static-loading test system, which can realize the artificial acceleration test under the coupling effect of fatigue load and complex environment at different scales, as shown in Fig. 4.

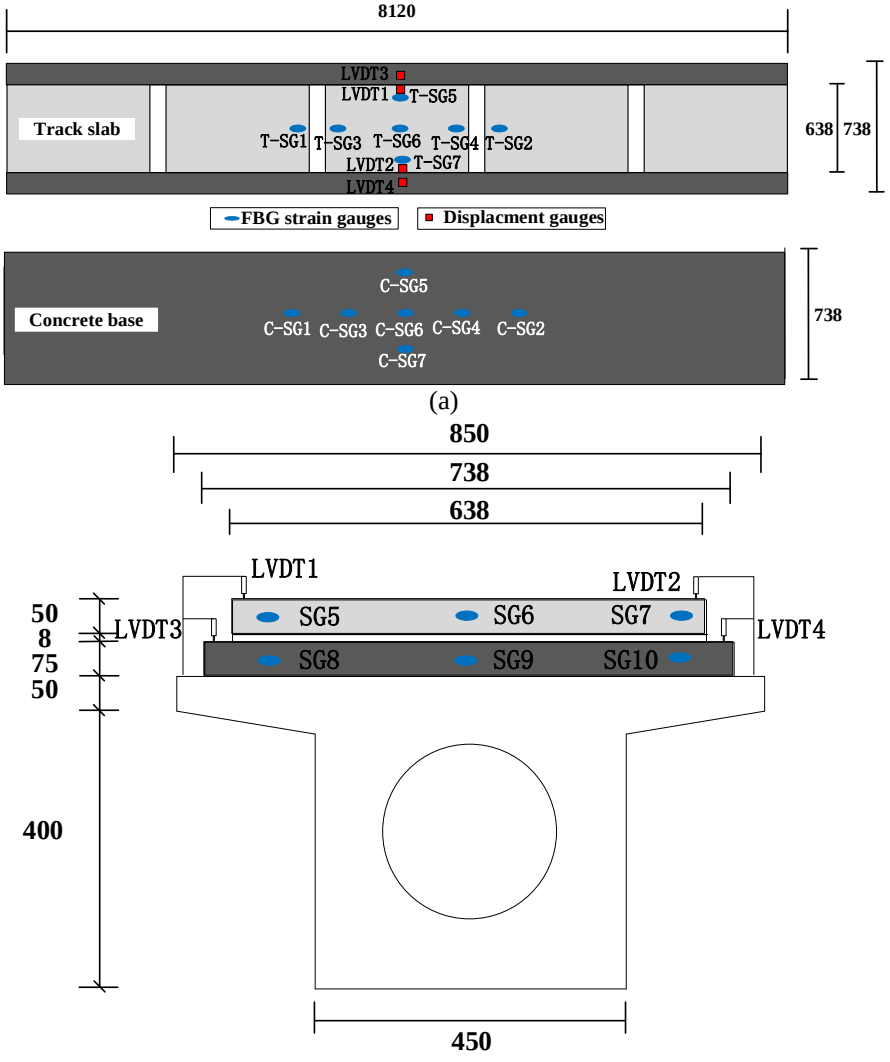

Figure (3): The sensors attached to the scaled specimen (unit: mm): (a) plan view of sensors; (b) vertical arrangement of sensors

Figure (4): Environment-load coupling test system

Loading Regime

The track-bridge structure system is simply supported at both ends, considering the longitudinal continuity characteristics of CRTS II slab ballastless track and the track structure was fixed at both ends (Cai et al., 2019). The loading method is shown in Fig. 5. According to the 2021 China Climate Bulletin, the extremely high temperature in south China and southwest China has exceeded the historical extreme value of 41°C. Based on the historical extreme temperature, 46°C was selected as the test environment temperature (Chen et al., 2021). In addition, to ensure the mechanical-fatigue consistency between the track-bridge structure system and the actual service environment, the upper limit of fatigue load was set to 45 kN and the lower limit was set to 25 kN and the load waveform is constant-amplitude sine-wave. Related studies have shown that the fatigue life of the specimen is no longer affected by the loading frequency when the loading frequency is in the range of 3 ~ 16 Hz (Du et al., 2020). As for the specimen in this work, the fatigue testing frequency was set as 5 Hz and the fatigue loading cycle was set to 1 million cycles, considering the exploitativeness and test period. After a certain number of fatigue cycles, static-load tests were carried out to collect displacement and strain data. The static-loading scheme is shown in Fig. 6.

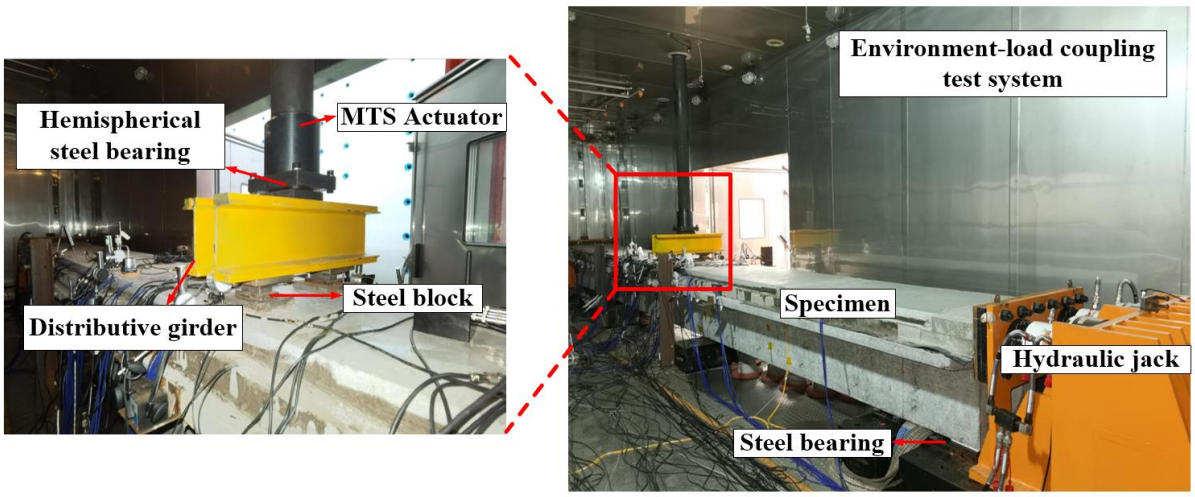

Figure (5): Laboratory setup of environment-load coupling tests

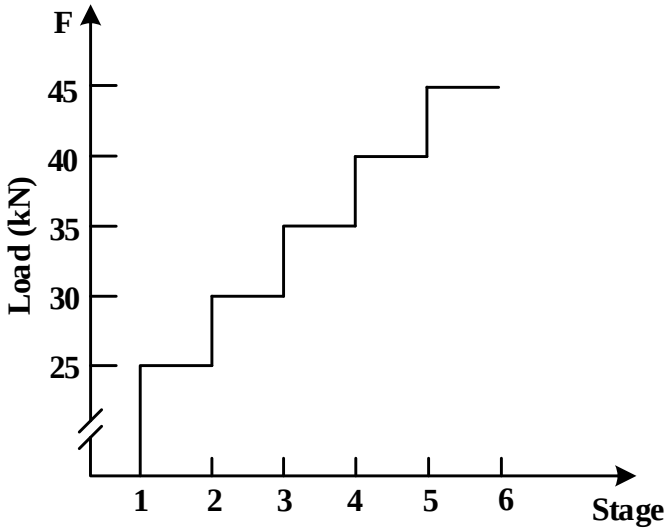

Figure (6): Static-loading test scheme

RESULTS AND DISCUSSION

Analysis of Static-deflection Results

During the cyclic loading test, the static loading test of the structure was carried out per 100000 cycles to obtain the load-disturbance variation laws in the mid-span of the track structure. In this paper, the evolution law of static disturbance of track structure under temperature-load coupling and train load was compared and analyzed, as shown in Fig. 7. As can be seen from Fig. 7, with the number of train load increasing, the static deflection of the structural system changes significantly and it is worth noting that the displacement continues to increase, the structure does not appear to crack and work performance remains intact. According to Fig. 7(a), under the single load (without considering the temperature loading), the load-displacement curves are scattered at the initial and final stages of cyclic loading, while they are denser at the middle stage of cyclic loading. This shows a three-stage characteristic "sparse-dense-sparse" behavior, with apparent linear correlation. According to Fig. 7 (b), compared with the former, when the temperature–load coupling was performed, the load-displacement curve of the structural system had an evident interval in the middle fatigue period and the static deflection value increased more significantly by approximately 14% at a static load of 25 kN. With the increase in cycle number, the slope of the load-deflection curve tended to decrease and the structural system slightly lost stiffness.

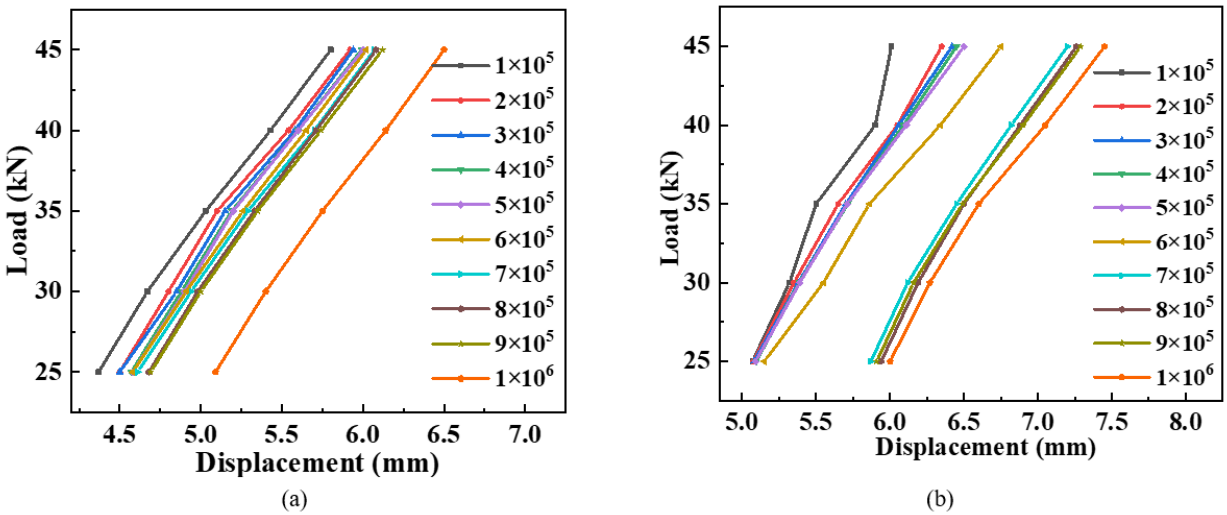

Figure (7): Loading-static deflection curves of the mid-span position of the track structure: (a) single load; (b) temperature-load coupling

Analysis of Dynamic Deflection Results

During the cyclic loading test, the dynamic deflection data was collected per 50,000 cycles and the dynamic deflection evolution curve of the structural system in the mid-span under the load was obtained, as shown in Fig. 8.

As observed from Fig. 8, the dynamic deflection of the structural system (without considering the temperature load) was 5.91 mm at the beginning of the cyclic load action and 6.13 mm at the end, with a 3.7% increase in the dynamic deflection; the dynamic deflection evolution process showed a slight tendency to increase. In addition, the dynamic deflection of the structural system under the coupled temperature-load action was 6.03 mm at the initial stage of the cyclic load action and 6.33 mm at the final stage, with a 5.0% increase in the dynamic disturbance. The dynamic deflection evolution process also showed a three-stage change of “slow-steep-slow”, which was different from the former three-stage change behavior. In summary, the dynamic deflection value of the structural system grew faster under the temperature-load coupling compared with that without considering the temperature load. The reason for this may be that the thermal coupling had a significant amplification effect on the structural dynamic deflection.

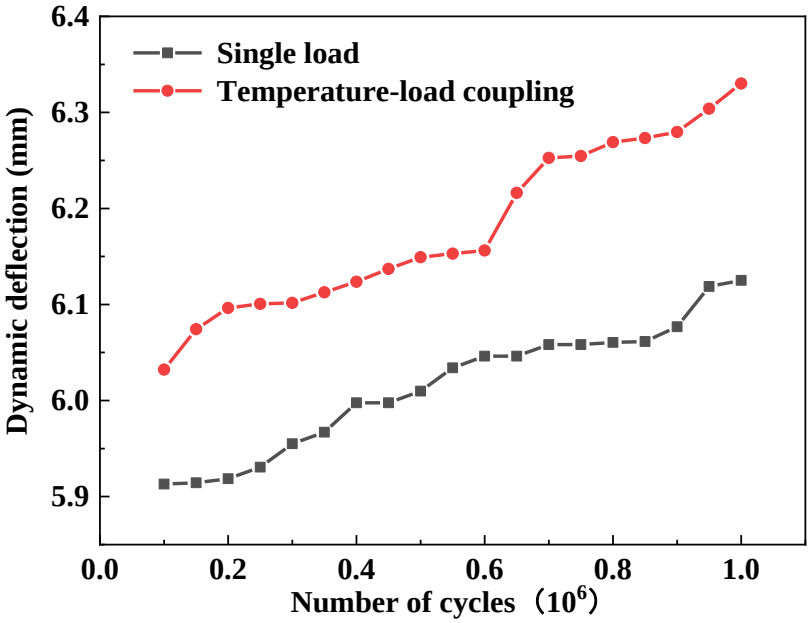

Figure (8): Dynamic deflection of mid-span

The Evolution of Structural Strain

There are no apparent cracks in the track structure system at the end of cyclic loading. The load-strain curves and test results of the longitudinal and transverse directions of the track slab and concrete base were analyzed as follows. In addition, the strain distribution under each load was similar. Since the strain distribution under each load was the same and space was limited, only the strain variation law of the track structure was listed when the static load was 45 kN.

The Strain of the Track Slab

The longitudinal and transverse load-strain curves of the track slab under constant amplitude fatigue loading are shown in Fig. 9. As the track slab was restrained at both ends, the track slab was squeezed by the restraining tooling at both ends under the load, mainly subjected to compressive stress. In this paper, the compressive stress was defined as "+" and the tensile stress was defined as "-", the same as below. This ndicated that the strain values of the structural layer of the track slab under different cycle times were symmetrically distributed. With the increasing number of cycle loading, the track slab increases in various degrees in both longitudinal and transverse positions. However, it should be noted that the strain values of the track slab under single load and temperature-load coupling vary considerably with the increase in the number of cyclic loading.

Figs. 9(a) and (b) show that the longitudinal strain value of the track slab varies relatively uniformly under a single load, with a maximum strain value variation of 33% and a minimum of 2.2% between adjacent loading times. However, the longitudinal mid-span strain value of the track slab under the coupled temperature-load effect was 54.5 με at the cyclic loading times of 1×10^5. When the loading times increased to 2×10^5, the mid-span strain value was 117.4 με, indicating an increase by 115%. The growth rate of the strain value gradually decreased with increasing cyclic loading times.

In Figs. 9(c) and (d), the rate of change of the transverse strain value of the track slab was similar to the rate of change of longitudinal strain. The strain value varied uniformly with a single load, while the strain value increased sharply during the cyclic loading times from 1×10^5 to 2×10^5. At the same time, it can be seen that the transverse strain distribution of the track slab under the two effects was different. The stress distribution of the track slab under a single load showd a concave shape, while the stress distribution under temperature-load coupling was convex. It is possible that the above test results are caused by the temperature core formed inside the track slab under the temperature load, resulting in temperature stress. Finally, the strain value in the middle of the track slab is greater than the strain value on both sides.

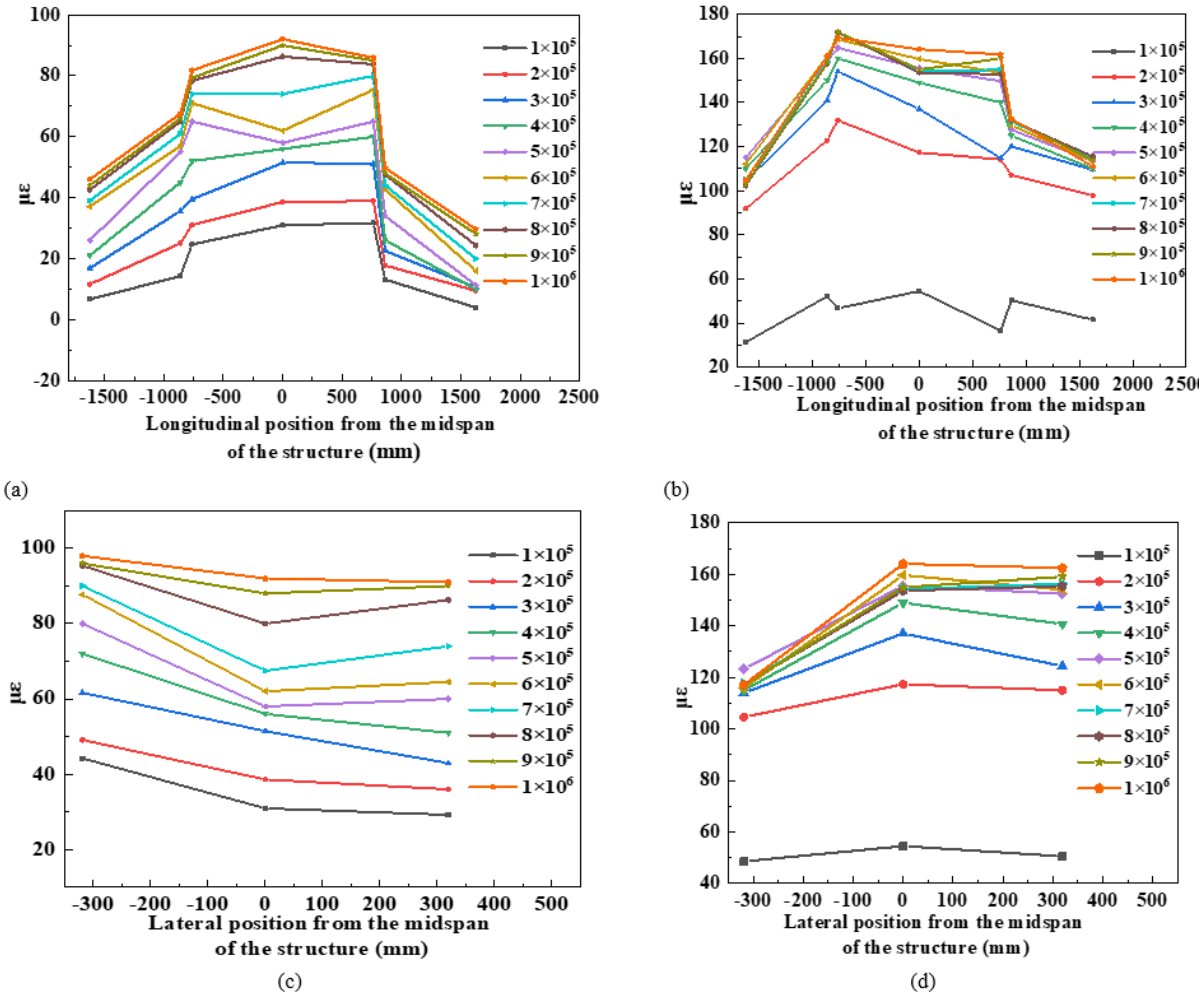

Figure (9): The law of strain evolution of track slab: (a) longitudinal strain under the single load; (b) longitudinal strain under the temperature-load coupling; (c) transverse strain under the single load; (d) transverse strain under the temperature-load coupling

The Strain of the Concrete Base

The longitudinal and transverse load-strain curves of the concrete base under constant amplitude fatigue loading are shown in Fig. 10. Due to the restraint at both ends of the concrete base, similar to the track slab, the structural layer of the concrete base is also subjected to compressive stresses under load. With the increasing number of cyclic loading, the strain value of the concrete base increases to different degrees under both single load and temperature-load coupling.

In Figs. 10(a) and (b), the overall variation in the longitudinal strain values between adjacent loading times under a single load was relatively uniform, with a maximum of 18% and a minimum of 2.4%. The rate of change of strain values under temperature-load coupling was different from that of a single load, with a sharp increase in strain values from 1×10^5 to 2×10^5 cyclic loading time, which is more than double the rate of change. The trend of the rate of change of the transverse strain value was analogous to that of the longitudinal strain value, as shown in Figs. 10(c) and (d). It is worth noting that the transverse stress distribution of the concrete base under single load and temperature-load coupling was similar to the transverse stress distribution corresponding to the track slab, both being caused by the large temperature stresses generated in the concrete base.

It can be seen that the concrete base and box beam middle laid two fabrics and a membrane (two layers of geotextile, a layer of plastic film) to form a sliding layer with a gap and the gap gradually compressed under the action of the load to fit and then eventually ballastless track and box beam to achieve cooperative bearing. Therefore, the cooperative bearing process of the

bridge-rail structure was more complex and with the uniform increase of the number of cycles, its strain value increases presenting a significant non-linearity, while there was an amplifying effect on the non-linearity under the temperature load. In addition, the presence of temperature stress in the concrete base was the main reason for the difference in transverse strain distribution.

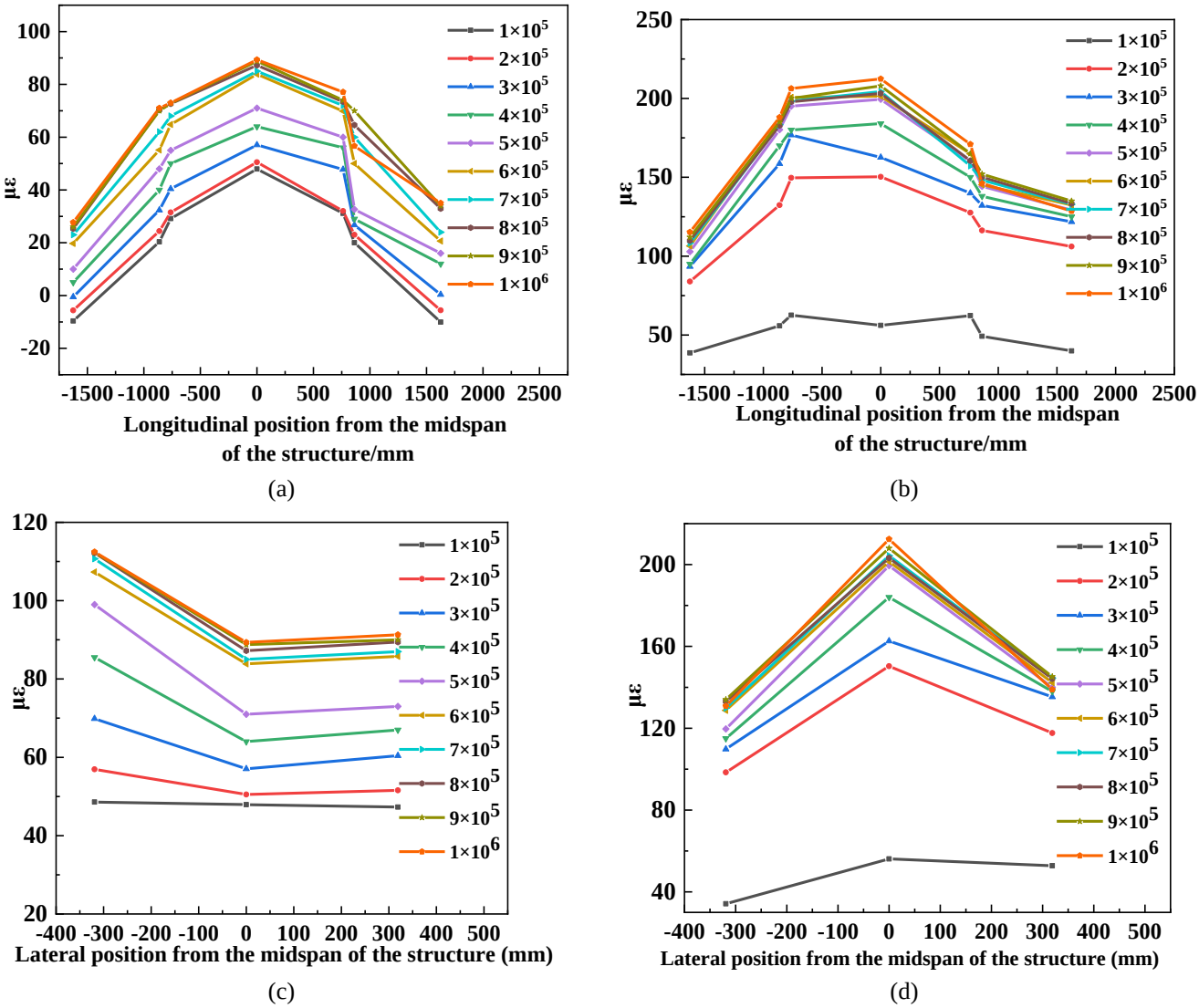

Figure (10): The law of strain evolution of concrete base: (a) longitudinal strain under the single load; (b) longitudinal strain under the temperature-load coupling; (c) transverse strain under the single load; (d) transverse strain under the temperature-load coupling

The Law of Temperature Effect on the Structural Dynamic Response

To investigate the dynamic response of the ballastless track-bridge under the action of different temperatures, an impulse test and a percussion test were carried out. In this paper, the vibration sensor and the supporting dynamic acquisition host were used for the test, while the vibration sensor was cemented to the corresponding position with an adhesive. The composition of the self-oscillation frequency acquisition system is shown in Fig. 11. Meanwhile, the hammer method of excitation was used in this paper to measure the excitation force and the response signal. The time course curves of the pulsation test and the time course curves of the percussion test were obtained at different temperatures (22℃~46℃). Due to space limitation, only the time course curves of the pulsation test and the percussion test under the structure temperature of 22℃ are shown in this paper, as in Figs. 12 and 13.

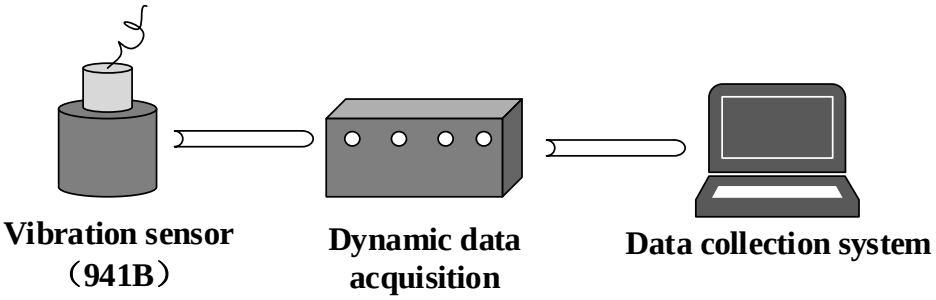

Figure (11): Self-vibration frequency acquisition system

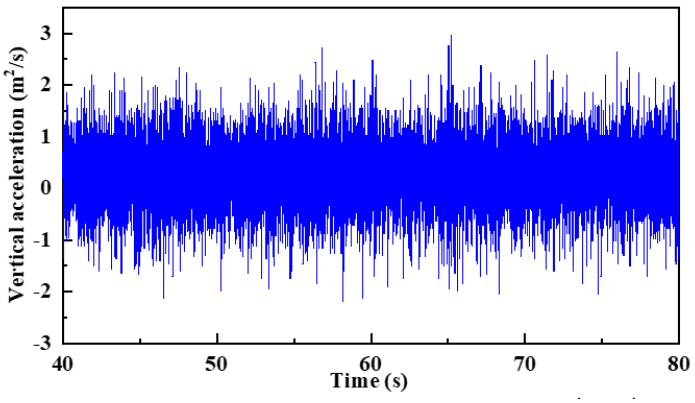

Figure (12): Time course curve of the pulsation test (22℃)

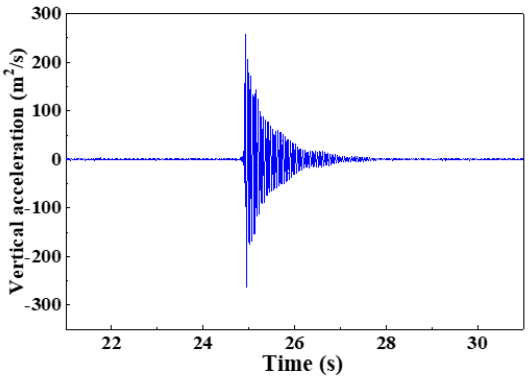

Figure (13): Time course curve of the percussion test（22℃）

Fast Fourier Transform (FFT) is one of the most widely used methods for frequency domain analysis of signals today. The FFT can be divided into FFT algorithm by time extraction and FFT algorithm by frequency extraction, with arranged parity for time-domain signal sequence and frequency-domain signal sequence, respectively (Guo et al., 2011). In this paper, the FFT algorithm by time extraction was used. The transform formula is shown in Equation. (1).

$$X[k] = X_1[k] + W_N^K X_2[k], k = 0,1,2\ldots\frac{N}{2} - 1 \quad (1)$$

Based on this, a fast Fourier transform of the acceleration time curve was applied to obtain the spectrum of the orbital structure under the effect of different temperatures, as shown in Fig. 14. Meanwhile, the analysis of the test results showed that when the temperature gradually increases, the inherent frequency of the track structure decreases to some extent, which indicates that temperature was also one of the crucial factors affecting the dynamic response of the track structure. Therefore, it was necessary for railroad workers to increase the supervision of track structures in high-temperature climates to further ensure the safety of track structure operations. In addition, the relationship between the intrinsic frequency and temperature in the track structure was illustrated in Fig. 15. The linear fitting method was used to fit the correlation and has great consistency with an R^2 approximately equal to 0.93. The relationship between the intrinsic frequency and temperature is shown in Equation (2).

$$F = 15.6 - 0.21T \quad (2)$$

where, F is the inherent frequency of the orbital structure, Hz; and T is the temperature of the orbital structure, °C.

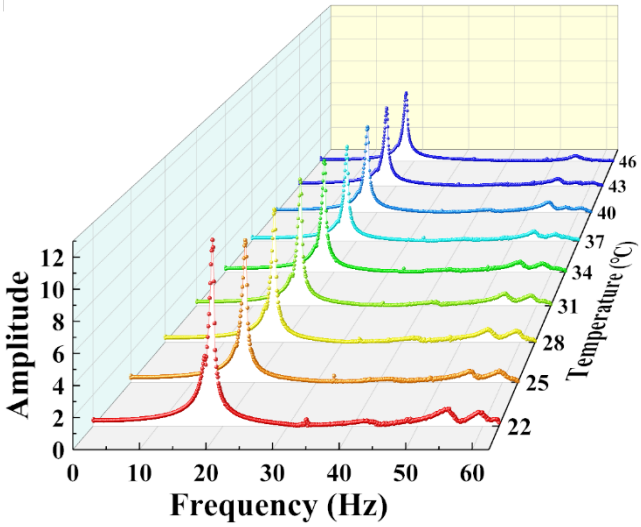

Figure (14): Frequency spectrum of track structure under different temperatures

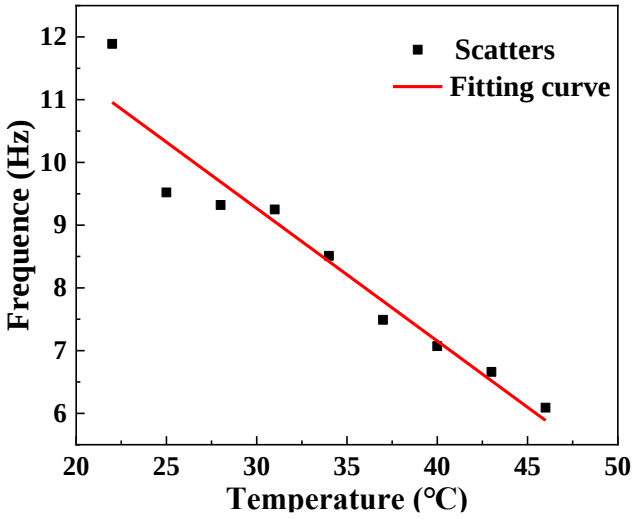

Figure (15): The relationship between the intrinsic frequency and temperature under different temperatures

Theoretical Verification

Fatigue tests were carried out for the above single-load and load-coupled effects, where the experimental results show that there is a degradation of the structural stiffness. To verify the stiffness degradation of the above structural fatigue test, this paper was based on the relationship between structural stiffness and impact coefficient as mentioned in the Chinese general design code for highway bridges and culverts (2015), as shown in the following equation:

$$\begin{cases} \mu = 0.05, \ f < 1.5Hz \\ \mu = 0.177Inf - 0.016, 1.5Hz \le f < 14Hz \\ \mu = 0.45, \ f \ge 14Hz \end{cases} \quad (3)$$

where, μ is the impact factor, f is the structural fundamental frequency. The fundamental frequency of the structure measured in this paper is between 1.5 Hz and 14 Hz.

In addition, combined with the Chinese highway bridge load test regulations (2015), the impact factor μ can be calculated according to the following formula:

$$\mu = \frac{f_d}{f_s} - 1 \quad (4)$$

where, f_d is the dynamic deflection and f_s is the static deflection.

According to Equations (2), (3) and (4), the impact factors μ of the design code and load test procedure were 0.39 and 0.23, respectively, while the theoretical calculation results were similar to the calculation results of the test procedure. The results showed that the theoretical calculation was in good agreement with the experimental results.

CONCLUSIONS

By means of the large test chamber with an environment-load coupling test system, single-load and temperature-load coupled load tests were conducted on 1/4 scale specimens of the ballastless track-bridge system. The main conclusions drawn can be summarized as follows:

(1) Without considering the temperature loading, the load-displacement curves showed a three-stage "sparse-dense-sparse" behavior with an apparent linear correlation. When temperature-load coupling was applied, the static disturbance of the load-displacement curve of the structural system increased significantly and the static disturbance increased by approximately 14% at a static load of 25 kN.

(2) Under the coupled temperature-load effect, the dynamic deflection of the structural system at the late loading stage increased by 16% compared with that at the early stage and the dynamic deflection evolution process showed a three-stage slow-steep-slow change, which was different from the

evolution of the dynamic deflection of the structural system without considering the temperature loading. The reason for this may have been that the thermal coupling had a significant amplification effect on the structural dynamic deflection.

(3) The cooperative bearing process of the track-bridge structure was more complex than the track structure and the maximum rate of change of the longitudinal strain value of the track slab is 33%, with a uniform increase in the number of cycles. There was an amplifying effect on the non-linearity under temperature loading and the strain value increased sharply between 1×10^5 and 2×10^5 cyclic loading times under coupling, whereas the strain of the track slab increased by 115%. The variation pattern of the strain values of the concrete base is similar to that of the track slab.

(4) As the temperature gradually increased, the inherent frequency of the track structure had a certain degree of reduction, which indicates that temperature is one of the essential factors affecting the dynamic response of the track structure. Railroad workers should increase the frequency of monitoring of track structure in high-temperature climates to protect the operational safety of the track structure.

Acknowledgments

The work described in this paper is supported by the National Natural Science Foundation of China (Grant Nos. 52178273 and 52278311), the Natural Science Foundation of Chongqing (Grant No. cstc2021jcyj-msxmX1159), the Chongqing Talent Plan Project (Grant No. cstc2022ycjh-bgzxm0124), the Chongqing Project of Joint Training Base Construction for Postgraduates (Grant No. JDLHPYJD2020004), the State Key Laboratory of Mountain Bridge and Tunnel Engineering (Grant Nos. SKLBT-YF2105 and SKLBT-ZD2101), Team Building Project for Graduate Tutors in Chongqing (Grant No. JDDSTD2022003) and Shenzhen Science and Technology Program (Grant No. GJHZ20220913143006012).

REFERENCES

Bose, T., Zania, V., and Levenberg, E. (2020). "Experimental investigation of a ballastless asphalt track mockup under vertical loads". Construction and Building Materials, 261, 119711.

Cai, X.P., Luo, B.C., Zhong, Y.L., Zhang, Y.L., and Hou, B.W. (2019). "Arching mechanism of the slab joints in CRTS II slab track under high-temperature conditions". Engineering Failure Analysis, 98, 95-108.

Chen, Y., Wang, L., Zhao, J.H., Zhang, Y.X., Zhao, S.S., Li, W., Zou, X.K., Jiang, Y.D., and Shi, S. (2022). "Climatic characteristics and major meteorological events over China in 2021". Meteorological Monthly, 48 (04), 470-478.

Chen, Z., Xiao, J.L., Liu, X.Y., and Qin, H.P. (2019). "Deformation behavior of slab warping for longitudinal continuous rigid slab under temperature effect". Advances in Structural Engineering, 22 (13), 2823-2836.

Dai, G.L., and Su, M. (2016). "Full-scale field experimental investigation on the interfacial shear capacity of continuous slab track structure". Archives of Civil and Mechanical Engineering, 16 (3), 485-493.

Du, Y.X., Wei, J., Yuan, J., Lai, Y.F., and Sun, D.H. (2020). "Experimental research on fatigue behavior of pre-stressed concrete beams under constant-amplitude and variable-amplitude fatigue loading". Construction and Building Materials, 259, 119852.

Feng, L.L., Jiang, L.Z., Zhou, W.B., Lai, Z.P., and Chai, X.L. (2019). "An analytical solution to the mapping relationship between bridge structures vertical deformation and rail deformation of high-speed railway". Steel and Composite Structures, 33 (2), 209-224.

Feng, Q.S., Sun, K., Chen, H.P., and Lei, X.Y. (2021). "Long-term prediction of fatigue crack growth in ballastless track of high-speed railway due to cyclic train load". Construction and Building Materials, 292, 123375.

Guo, G., Li, Z., Li, J.J., and Hu, L.Y. (2011). "Realization of 128-point sampling data real-time FFT based on ATmega64L MCU". Radio Engineering, 41 (03), 53-55.

Jiang, L.Z., Feng, L.L., Zhou, W.B., and He, B.B. (2019). "Vibration characteristic analysis of high-speed railway simply supported beam bridge-track structure system". Steel and Composite Structures, 31 (6), 591-600.

Li, Y., Chen, J.J., Wang, J.X., Shi, X.F., and Chen, L. (2020). "Analysis of damage of joints in CRTSII slab track under temperature and vehicle loads". KSCE Journal of Civil Engineering, 24 (4),1209-1218.

Liu, X., Zhao, P.R., and Dai, F. (2011). "Advances in design theories of high-speed railway ballastless tracks". Journal of Modern Transport, 19 (3), 154-162.

Liu, X.K., Zhang, W.H., Xiao, J.L., Liu, X.Y., and Li, W. (2019). "Damage mechanism of broad-narrow joint of CRTS II slab track under temperature rise". KSCE Journal of Civil Engineering, 23 (5), 2126-2135.

Lou, P., Zhu, J.P., Dai, G.L., and Yan, B. (2018). "Experimental study on bridge-track system temperature actions for Chinese high-speed railway". Archives of Civil and Mechanical Engineering, 18 (2), 451-464.

National Standards of PRC. (2015). "General specifications for design of highway bridges and culverts". JTG D60-2015.

National Standards of PRC. (2015). "Highway bridge load test regulations". JTG/T J21-01-2015.

Ou, Z.M., and Li, F.J. (2014). "Analysis and prediction of the temperature field based on *in-situ* measured temperature for CRTS-II ballastless track". Procedia-Energy, 61, 1290-1293.

Ren, J.J., Tian, G.Y., Xu, J.D., Deng, S.J., and Xie, P. (2019). "Load effect -and fatigue-life prediction of prefabricated slab track for mixed passenger and freight railway". Journal of the China Railway Society, 41 (3), 110-116.

Sheng, X.W., Zheng, W.Q., Zhu, Z.H., Qin, Y.P., and Guo, J.G. (2020). "Full-scale fatigue test of unit-plate ballastless track laid on long-span cable-stayed bridge". Construction and Building Materials, 247, 118601.

Song, A.X., Yao, G.W., Yu, X.R., Wang, Y.R., and Wu, Y.F. (2022). "Experimental study and numerical analysis of structural performance of CRTS II slab track under extremely high temperatures". Advances in Materials Science and Engineering, 2022.

Song, A.X., Yao, G.W., Zhou, R., Yu, X.R., Wang, Y.R., and Guo, Q. (2023). "Experimental and numerical investigations of structural performance of CRTS II slab track under the hygrothermal environment". Jordan Journal of Civil Engineering, 17 (1),117-133.

Tarifa, M., Zhang, X.X., Ruiz, G., and Poveda, E. (2015). "Full-scale fatigue tests of precast reinforced concrete slabs for railway tracks". Engineering Structures, 100, 610-621.

Wang, J.F., Zhou, Y.B., Wu, T.M., and Wu, X. (2019). "Performance of cement asphalt mortar in ballastless slab track over high-speed railway under extreme climate conditions". International Journal of Geomechanics, 19 (5), 04019037.1-04019037.11.

Yang, R.S., Li, J.L., Kang, W.X., Liu, X.Y., and Cao, S.H. (2017). "Temperature characteristics analysis of the ballastless track under continuous hot weather". Journal of Transportation Engineering, Part A: Systems, 143 (9), 04017048.1-04017048.10.

Zeng, Z.P., Wang, J.D., Shen, S.W., Li, P., Abdulmumin, A.S., and Wang, W.D. (2019). "Experimental study on evolution of mechanical properties of CRTS III ballastless slab track under fatigue load". Construction and Building Materials, 210, 639-649.

Zhang, G.C., Zhou, L.Y., Wei, T.Y., Yang, L.Q., Zhao, L., and Zeng, Y.H. (2021). "Mechanical performance of CRTS II ballastless track-bridge structural system under static load". Journal of Central South University (Science and Technology), 52 (5), 1712-1723.

Zhao, L., Zhou, L.Y., Zhang, Y.Y., Yuan, Y.H., Zou, L.F., and Yu, Z.W. (2021). "Experimental study on temperature distribution of CRTS II ballastless track on high-speed railway bridge in summer". Journal of Railway Science and Engineering, 18 (2), 287-296.

Zhou, L.Y., Zhao, L., Zhang, G.C., Wei, T.Y, Zeng, Y.H., and Peng, X.S. (2020). "Model test study on CRTS II ballastless track under rapid temperature rise and fall on high-speed railway bridge". Journal of the China Railway Society, 42 (4), 90-98.

Zhou, R., Zhu, X., Ren, W.X., Zhou, Z.X., Yao, G.W., Ma. C., and Du, Y.L. (2022). "Thermal evolution of CRTS II slab track under various environmental temperatures: Experimental study". Construction and Building Materials, 325, 126699.

Zhu, S.Y., and Cai, C.B. (2014). "Interface damage and its effect on vibrations of slab track under temperature and vehicle dynamic loads". International Journal of Non-linear Mechanics, 58, 222-232.